The Astrophysical Journal Supplement Series, 202:16 (6pp), 2012 October doi:10.1088/0067-0049/202/2/16

SCALER MODE OF THE AUGER OBSERVATORY AND SUNSPOTS

Carlos A. García Canal[1], Carlos Hojvat[2], and Tatiana Tarutina[1]
[1] Instituto de Física La Plata, CCT La Plata, CONICET and Departamento de Física, Facultad de Ciencias Exactas, Universidad Nacional de La Plata CC 67, 1900 La Plata, Argentina
[2] Fermilab, P.O. Box 500, Batavia, IL 60510-0500, USA
Received 2012 April 11; accepted 2012 August 26; published 2012 September 20

ABSTRACT

Recent data from the Auger Observatory on low-energy secondary cosmic ray particles are analyzed to study temporal correlations together with data on the daily sunspot numbers and neutron monitor data. Standard spectral analysis demonstrates that the available data show $1/f^{\beta}$ fluctuations with $\beta \approx 1$ in the low-frequency range. All data behave like Brownian fluctuations in the high-frequency range. The existence of long-range correlations in the data was confirmed by detrended fluctuation analysis. The real data confirmed the correlation between the scaling exponent of the detrended analysis and the exponent of the spectral analysis.

Key words: methods: statistical – sunspots

Online-only material: color figures

1. INTRODUCTION

Solar activity gives rise to a modulation of the flux of cosmic rays observed from Earth. The Pierre Auger Observatory (Auger Collaboration 2004) has made available the scaler singles rates observed on their surface detectors reflecting the counting rates of low-energy secondary cosmic-ray particles (Pierre Auger Collaboration 2008, 2011; Dasso et al. 2012). These data are presented after corrections for atmospheric effects, pressure in particular, and compared with temporal variations of solar activity as shown by data obtained with neutron monitors (Neutron Monitor Database 2011). Solar and cosmic-ray data can be presented as a temporal series containing modulations, correlations, and noise fluctuations. The availability of Auger scaler data and data from neutron monitors as well as sunspot numbers (SIDC-Team 2011) motivated us to study the existence of long-range correlations present in the corresponding time series.

The Pierre Auger Observatory is located in the city of Malargüe, Mendoza, Argentina. In order to study the highest energy cosmic rays, it covers a surface of 3000 square kilometers with 1600 surface detectors sensitive to the transversal distributions of the showers generated by the primary cosmic rays. In addition, the longitudinal shower development is measured via atmospheric fluorescence using 27 optical telescopes. To monitor performance, the surface detectors have scalers that record signals received above a given threshold independent of any further shower reconstruction involving other neighboring detectors. This is referred to as the "scaler mode" of the Auger surface detector. The low threshold rates, or scaler data, have been recorded by the surface detectors of Auger Observatory since 2005 March. These data should be sensitive to transient events such as gamma-ray bursts and solar flares. The rates at each detector are registered every second and the 15 minute average rates are publicly available (Auger Scaler Data Online 2011). The temporal variations can be accurately studied, as these rates are very large as compared to other data on solar activity.

In the work of the Pierre Auger Collaboration (2011), the pressure-corrected Auger scalers were compared to data from the Rome neutron monitor (Storini et al.) and it was concluded that Auger scalers could be suitable for the study of solar activity.

A sunspot is a temporary phenomenon in the solar photosphere that appears like a dark visible spot compared to the surrounding regions (see, for example, Bray & Loughhead 1979). It corresponds to a relatively cool area of the Sun photosphere (1500 K less than the average photosphere temperature) as a result of the heat convection process inhibition by intense magnetic fields.

The number of sunspots and their position on the Sun change with time as a consequence of solar cycle activity. The maximum solar activity corresponds to a large number of sunspots and less sunspots are observed in the minimum. The spots usually appear in groups.

Data on sunspots are available for the last four centuries. From 1749 to 1981 the sunspot data were provided by the Zürich Observatory. Presently, the World Data Center for the Sunspot Index in the Royal Observatory of Belgium is responsible for recording sunspot data. All data are available online (SIDC-Team 2011).

Neutron monitors are ground-based detectors that measure the flux of cosmic rays from the Sun and low-energy cosmic rays from elsewhere in the universe. In a typical neutron monitor, low-energy neutrons produced by nuclear reactions in lead are slowed down to thermal energies by a moderator and detected by proportional counter tubes. A worldwide network consisting of approximately 50 stations is in operation and their data are available online (Neutron Monitor Database 2011).

For this analysis we select data from two neutron monitoring stations. The sites were chosen for the availability of complete data for the entire period of availability of Auger scaler data. Therefore, there was no necessity to perform an interpolation procedure. These two neutron monitors are known as JUNG (Neutron Monitor JUNG) and APTY (Neutron Monitor APTY). The JUNG detector is located on top of the Sphinx Observatory Jungfraujoch, Switzerland and APTY is situated in the town of Apatity, Russia.

The aim of this paper is to present a systematic analysis of the temporal series from different experimental determinations. This analysis, based on power spectra behavior (Fanchiotti et al. 2004) and detrended power behavior (Peng et al. 1994; Fanchiotti et al. 2004), allows us to gain quantitative information about correlations among the different phenomena. It is also

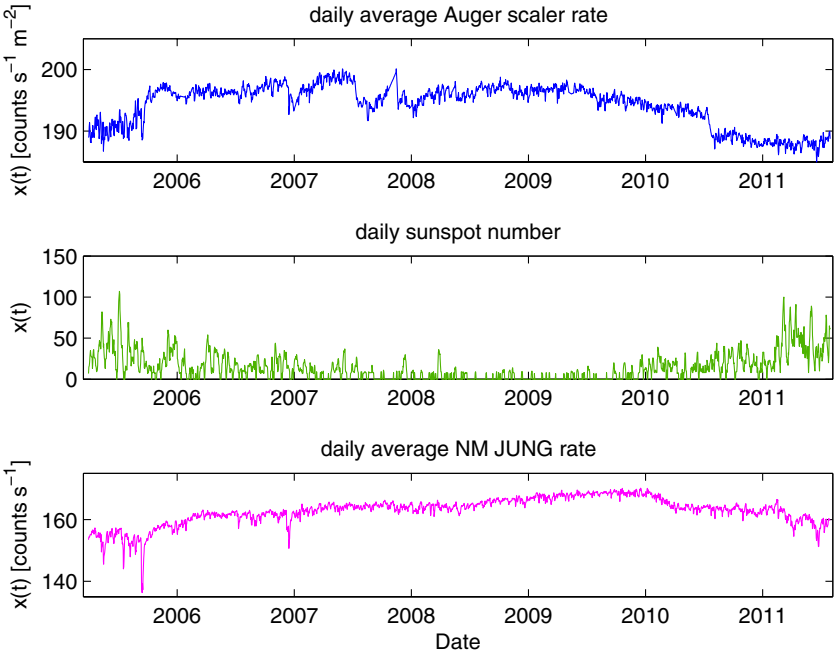

Figure 1. Auger scalers, sunspots, and neutron monitor JUNG data.
(A color version of this figure is available in the online journal.)

interesting to study the connection between the information provided by the power spectra analysis and the detrended analysis for the case of real data.

This paper is organized as follows: in Section 2 we present the results of the power spectra analysis of the three data sets and in Section 3 we present the results of the corresponding detrended analysis. Final remarks are given in Section 4.

2. POWER SPECTRA

There are a number of acceptable techniques (Hamilton 1994) for characterizing random processes $x(t)$. Usually, one starts with the correlation function defined as

$$G(\tau) = \langle x(t_0)x(t_0+\tau)\rangle_{t_0} - \langle x(t_0)\rangle^2_{t_0}. \quad (1)$$

Another widely used tool is the frequency spectrum which is defined as the squared amplitude of the Fourier transform of the time signal:

$$S(f) = \lim_{T\to\infty} \frac{1}{T}\left|\int_{-T}^{T} d\tau x(t) e^{2i\pi f\tau}\right|^2. \quad (2)$$

For a stationary process, the frequency spectrum is connected with the temporal correlation function through the Wiener–Khintchine relation (MacDonald 1962):

$$S(f) = 2\int_0^\infty d\tau G(\tau)\cos(2\pi f\tau). \quad (3)$$

A true random process, also called white noise, has no correlations in time, therefore the correlation function for the white noise is a delta function and the spectrum function $S(f) \propto$ const. The Brownian motion (MacDonald 1962) or random walk corresponds to the spectrum function $S(f) \propto 1/f^2$.

Many naturally occurring fluctuations of physical, astronomical, biological, economic, traffic, and musical quantities exhibit $S(f) \propto 1/f$ behavior over all measured timescales (see, for example, Voss & Clarke 1975; Press 1978; Matthaeus & Goldstein 1986; Van Vliet 1991; Baillie 1996; Novikov et al. 1997). These fluctuations are of interest because they correspond to the existence of extremely long-range time correlations in the time signals. This can be shown (see Jensen 1998) if one assumes that the spectral function of a time signal $S(f) \propto 1/f^\beta$ and that the temporal correlation function $G(\tau) \propto 1/\tau^\alpha$. It follows from Equation (3) that $1/f^\beta \propto 1/\tau^{1-\alpha}$. When $\beta \approx 1$ it follows that $\alpha \approx 0$ which corresponds to correlation function $G(\tau) \approx 1$.

An analysis of monthly sunspot data was performed in the work of Fanchiotti et al. (2004), including the study of the power spectra and detrended analysis. It was found that the high-frequency part of the spectral function of the monthly sunspots shows $1/f^\beta$ behavior with $\beta = 0.8 \pm 0.2$. This corresponds to $1/f$ noise.

In Figure 1 we present the available time series data obtained as indicated in the corresponding references: (1) Auger scalers (Auger Scaler Data Online 2011), (2) sunspots (SIDC-Team 2011), and (3) JUNG neutron monitor data (Neutron Monitor Database 2011) for the time period when data on the Auger scalers are available. As the Auger scalers contained gaps, sometimes of several days, in order to use them in the analysis we performed an interpolation of the data justified by the Brownian behavior of data for the high frequencies.

In Figure 2 we present the power spectra of available data on a logarithmic scale versus frequency. The power spectra for the sunspots and the neutron monitor were shifted with respect to each other to avoid overlap. The spectral function indicates the presence of two different behaviors for low and high frequencies that can be approximated by linear function with the smaller slope in the lower frequency range. The frequency corresponding to the change from one region to another is different for each data set. We also note that in the sunspot daily spectra there is a peak corresponding to the frequency of approximately $1/27 = 0.04\ \text{day}^{-1}$, not clearly seen in Figure 2 because of the low statistics. This 27 day peak is

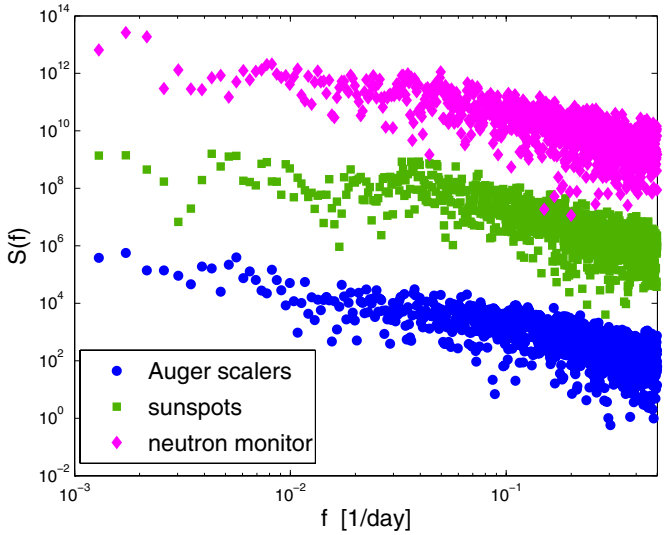

Figure 2. Power spectra of daily Auger scalers, sunspots, and the neutron monitor JUNG.

(A color version of this figure is available in the online journal.)

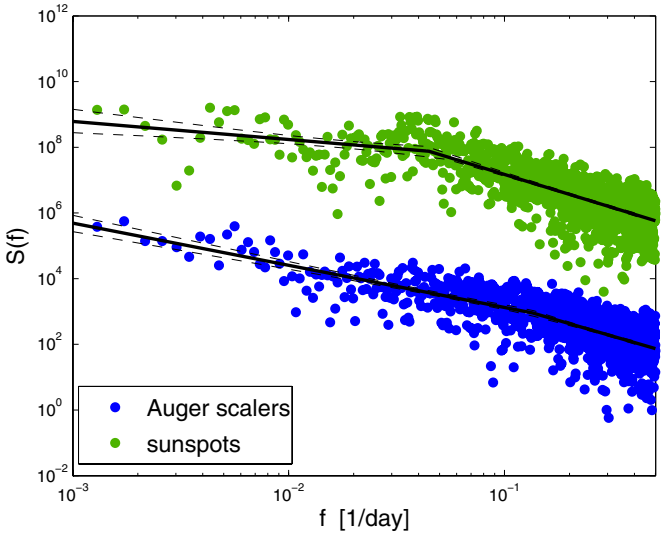

Figure 3. Power spectra of daily Auger scalers and sunspots with the corresponding result of the fit with piecewise linear function (solid lines). Dashed lines indicate 95% prediction bounds.

(A color version of this figure is available in the online journal.)

Table 1

Values of β for Different Frequency Ranges Obtained by Fitting the Power Spectra with a Piecewise Linear Function with f_c as a Free Parameter in the Fit

Quantity	Auger Scalers	Sunspots	NM JUNG	NM APTY
$\log(f_c/\text{day}^{-1})$	-0.87	-1.35	-1.25	-1.15
β total f range	1.525 ± 0.073	1.591 ± 0.080	1.564 ± 0.078	1.549 ± 0.079
β low f	1.28 ± 0.14	0.55 ± 0.32	1.12 ± 0.23	1.11 ± 0.22
β high f	1.91 ± 0.23	2.02 ± 0.13	1.79 ± 0.14	1.86 ± 0.16

due to solar rotation (Bray & Loughhead 1979). At first sight the description with the piecewise linear function seems more justified for the spectral function of the sunspots than in the spectral function of the scalers which shows more attenuated behavior for relatively small frequencies. In addition, the slope for the low-frequency part of the spectrum for the Auger scalers and the neutron monitor is smaller compared with that of the sunspots. We further analyze these facts below.

We analyzed the power spectra of Auger scalers, sunspots, and two neutron monitors using a linear least-squares fit. First, we fitted the data for the total range of frequencies. The resulting β is presented in the third line of Table 1. All data have similar slopes when fitted over the total range of frequencies, giving $\beta \approx 1.6$.

Second, we performed a fit of the data to the piecewise linear function consisting of two parts with different slopes. The frequency corresponding to the point of change of the slope f_c was adjusted independently for each data set to obtain the best fit and is presented in the second line of Table 1. The fitted values of β for the range of low frequencies are given in the fourth line and for high frequencies in the fifth line. In Figure 3 we present the results of the fitting for Auger scalers and sunspots.

It is seen from this analysis that in the low-frequency range all data show the existence of long-range correlations with $\beta \approx 1$. For high frequencies, the spectral function shows Brownian behavior. It is also seen that the position of f_c is different for each data set. It should be noted that in the case of sunspots the position of f_c could be dictated by the 27 day cycle of solar activity (Bray & Loughhead 1979).

In order to have more quantitative conclusions about the value of β, we performed a systematic fit of all data for different frequency ranges. In this analysis we set various sizes of the considered frequency intervals $[10^{-3}\ \text{day}^{-1}, f_i]$ with $f_i = 10^{-2}\ \text{day}^{-1} + \Delta f$ up to approximately f_c with $\Delta f = 10^{0.2}$ day^{-1} and present the fitted slope β for sunspots, Auger scalers, and the neutron monitor JUNG in Figure 4(a). For $f_i \approx 10^{-1}$ day^{-1}, all sets of data in the range of low frequencies, namely $10^{-3}\ \text{day}^{-1} < f < f_c$, are fit, $\beta \approx 1$. In the case of sunspots for $f \approx 0.04\ \text{day}^{-1}$ the drop in β can be explained by the influence of the aforementioned 27 day peak which is not seen in the case of Auger scalers and neutron monitors. For smaller frequencies the error is large for all the data because of the low statistics but the results agree within the error bars.

In Figure 4(b) we show the results of a similar analysis but this time for the range of high frequencies. Here we obtain the value of β fitting the spectral function over the frequency interval with varying size $[f_j, f_N]$, where $f_j = f_N - \Delta f$ with Δf as before, and f_N stands for the Nyquist frequency. It is seen that for $f_j \approx 10^{-1}\ \text{day}^{-1}$ all the data predict a similar value of β. As f_j approaches $10^{-2}\ \text{day}^{-1}$ its value drops because of the influence of the part of the low-frequency spectra.

For the high-frequency range, the data show agreement with the following behavior:

$$S(f) \approx f^{-1.9\pm0.2}, \tag{4}$$

which corresponds to Brownian fluctuations. This is an expected behavior because at high frequencies the fluctuations become more random or less correlated.

We can conclude that the data show the coexistence of two behaviors in the power spectra: (1) consistent with a $1/f$ dependence for low frequencies and (2) consistent with a $1/f^2$ behavior for high frequencies. Our analysis confirms the result of Fanchiotti et al. (2004) where monthly data on the sunspots were analyzed. The sunspots in this frequency region have $1/f$ behavior. The $1/f^2$ behavior was not detected in Fanchiotti et al. (2004) because it corresponds to the high frequencies which are not present in monthly data.

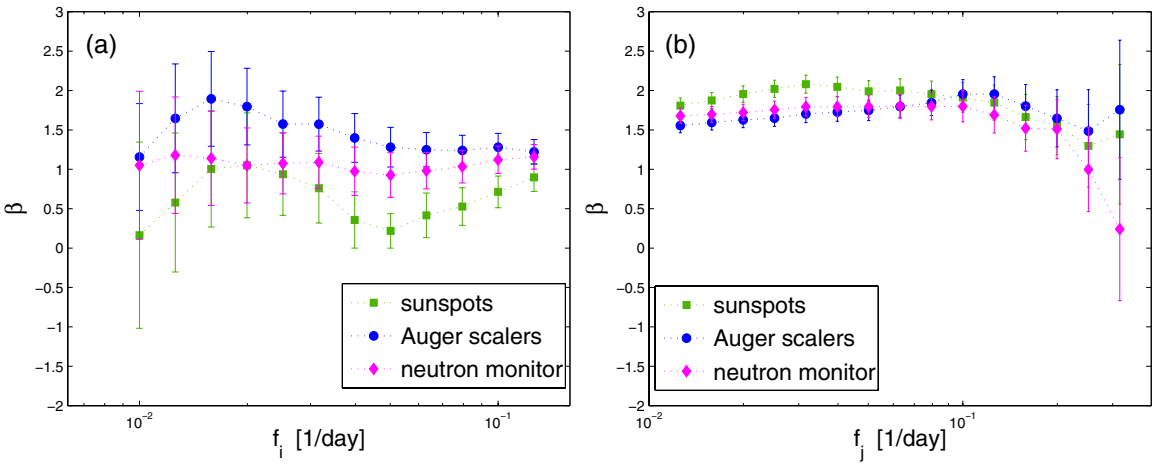

Figure 4. Dependence of the power spectra slope β on the range of frequency used for the fit: (a) low-frequency range; (b) high-frequency range. See the text for explanation. The dotted lines are to guide the eye.

(A color version of this figure is available in the online journal.)

3. DETRENDED FLUCTUATION ANALYSIS

Another statistical method to reveal the extent of long-range temporal correlations in a time series is detrended fluctuation analysis (DFA). This method was introduced in Peng et al. (1994) and applied in many areas of research, including physical and biological sciences.

Consider the time series $x(t)$ consisting of N samples. The procedure is as follows:

1. First, generate a new time series $u(t_n)$ by means of

$$u(t_n) = \sum_{k=1}^{n} x(t_k), \quad u(0) = 0, \quad n = 1, \ldots, N. \qquad (5)$$

2. Divide the time series $u(t)$ into non-overlapping intervals of equal length s. In each interval the data are fitted to the first-order polynomial using least squares (the polynomial of second or third order may be used as well; see Kantelhardt et al. 2002), giving a local trend $y(t) = at + b$.
3. In each interval, calculate the detrended fluctuation function using

$$[F(s)]^2 = \sum_{t=ks+1}^{(k+1)s} [u(t) - y(t)]^2; \quad k = 0, 1, \ldots, \left(\frac{N}{s} - 1\right).$$

4. Calculate the average of $F(s)$ over N/s intervals.

For a fluctuating time series, the expected behavior is as follows:

$$\langle F(s) \rangle \sim s^{\mathrm{H}_\alpha},$$

where H_α is a scaling exponent, a generalization of the Hurst exponent (Kantelhardt et al. 2002).

Initially, the DFA was proposed as an independent measure of long-term correlation, complementary to spectral analysis information. In the work of Buldyrev et al. (1995, p. 5089) it was noted that the value of β of the spectral function and $\beta' = 2\mathrm{H}_\alpha - 1$ are "remarkably close to each other." In this analysis $\mathrm{H}_\alpha = 1/2$ corresponds to the case of white noise, $1/2 < \mathrm{H}_\alpha < 1$ reveals the existence of positive correlations, and the special case when $\mathrm{H}_\alpha = 1$ corresponds to $1/f$ noise. Random walk is characterized by $\mathrm{H}_\alpha = 3/2$. Heneghan & McDarby (2000) examined the analytical link between DFA and spectral analysis and showed that they are related through an integral transform. It was concluded that DFA and spectral measures provide equivalent characterizations of stochastic signals with long-term correlation. In this work we study the connection between the scaling exponent H_α and the coefficient β introduced in the spectral function analysis to check this assertion in this particular case with the real data.

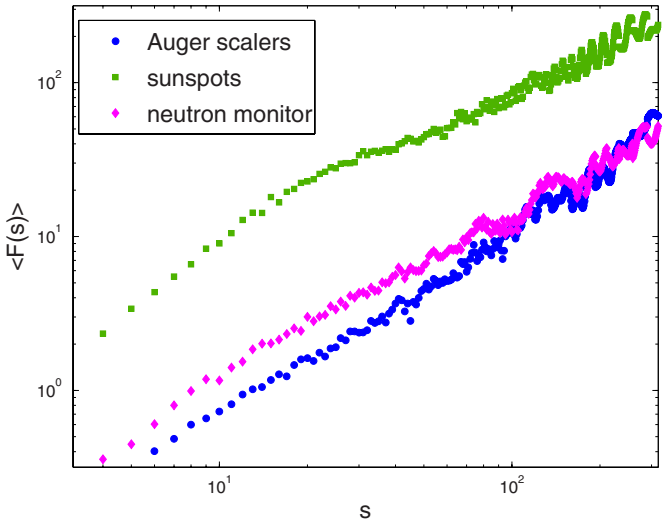

Figure 5. Detrended fluctuation analysis curves of Auger scalers, sunspots, and neutron monitor JUNG.

(A color version of this figure is available in the online journal.)

In Figure 5 the results of the DFA of Auger scalers, sunspot numbers, and one neutron monitor (JUNG) are shown. In the case of the sunspots, the data can be separated into three regions with different slopes: (a) $s \lesssim s_c$, (b) $s_c \lesssim s \lesssim 10^2$, and $s \gtrsim 10^2$ (the numbers here are approximate). The value of s_c in the case of sunspots approximately corresponds to the 27 day peak in the spectral function. For the case of Auger scalers and neutron monitors the existence of three regions in the DFA curve is not as clear as in the case of the sunspots but a close examination of Figure 5 suggests a change of slope at $s \approx 10$ for Auger scalers and neutron monitors. The situation is similar to the power spectra curves where the difference between the regions with $1/f$ and $1/f^2$ is more apparent for the case of the sunspots.

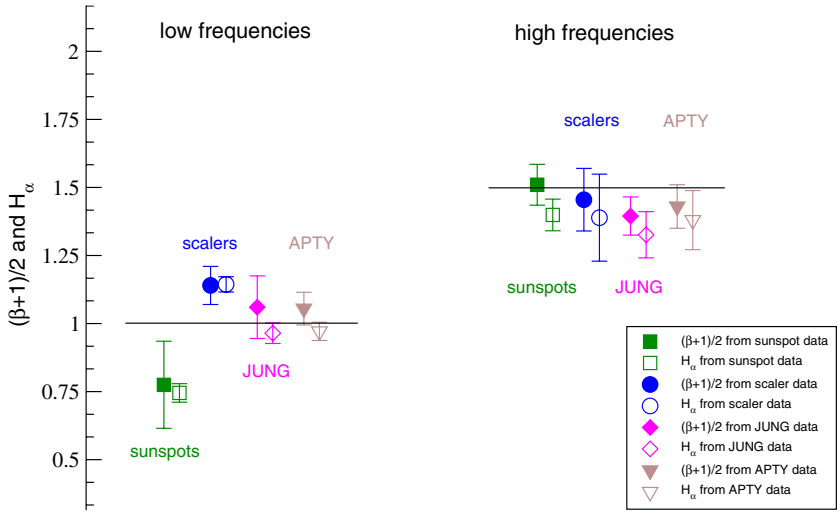

Figure 6. Comparison between $(\beta + 1)/2$ and the scaling exponent H_α for sunspot, Auger scaler, and neutron monitor data calculated in the regions of high and low frequencies.

(A color version of this figure is available in the online journal.)

Table 2
The Result of the Spectra Analysis $(\beta + 1)/2$ and the Scaling Exponent H_α for Sunspots, Auger Scalers and Two Neutron Monitors

Frequency	β	$(\beta + 1)/2$	H_α
	Sunspots		
High	2.02 ± 0.13	1.51 ± 0.08	1.40 ± 0.06
Low	0.55 ± 0.32	0.78 ± 0.16	0.75 ± 0.03
	Auger scalers		
High	1.91 ± 0.23	1.46 ± 0.12	1.39 ± 0.16
Low	1.28 ± 0.14	1.14 ± 0.07	1.14 ± 0.03
	NM JUNG		
High	1.79 ± 0.14	1.40 ± 0.07	1.33 ± 0.09
Low	1.12 ± 0.23	1.06 ± 0.12	0.96 ± 0.04
	NM APTY		
High	1.86 ± 0.16	1.43 ± 0.08	1.38 ± 0.11
Low	1.11 ± 0.22	1.06 ± 0.06	0.97 ± 0.03

There is a correspondence between the frequency in the power spectra of the time series and the value of s. The region of large values of s corresponds to the very small frequencies of the time series and have large fluctuations that can be seen in Figure 5. This region of large values of s is excluded from our analysis.

In Table 2 we compare the exponent β, and $(\beta + 1)/2$, with the coefficient H_α which characterized the slope obtained in the DFA analysis for two ranges of the frequencies: (a) "high frequency" $s \lesssim s_c$ and (b) "low frequency" $s_c \lesssim s \lesssim 10^2$, where $\log(s_c)$ is taken as equal to the modulus of the logarithm of the frequency corresponding to the change of the regimen in the power spectra (and given in Table 1). First of all, it is seen that the calculated scaling exponent for low frequencies is always $H_\alpha \approx 1$ which implies the existence of long-range correlations. It should be noted that the analysis of the daily sunspot numbers confirmed the result of the analysis of the monthly sunspot number performed by Fanchiotti et al. (2004), where the value obtained for the scaling exponent was $H_\alpha = 0.62 \pm 0.4$. This corresponds to the low frequencies as the high frequencies are not seen in the monthly data.

In order to compare the results of power spectra analysis and DFA we present in Figure 6 the slopes calculated using these two methods with the error bars indicated. The results are grouped by frequency: to the left for low frequencies and to the right for high frequencies. In each of these groups we present the resulting $(\beta + 1)/2$ from spectral analysis (filled markers) and the scaling exponent from DFA (open markers). It is seen that the results of both methods agree within the error bars and are consistent with $H_\alpha \approx 1$ for low frequencies and $H_\alpha \approx 3/2$ for high frequencies. Thus, in this work using real data from three different sources we confirm the correspondence between the value of β of the spectral function and the scaling exponent of DFA for both frequency ranges.

4. FINAL REMARKS

We have presented a statistical study of the available data on Auger scalers, sunspots, and neutron monitors. We studied the frequency spectra and performed a detrended analysis. We found that the spectral function can be separated into two regions: (1) the region of low frequencies and (2) the region of high frequencies that can be described by power laws. It was shown that the low-frequency part of the spectral function of all data shows $1/f$ behavior. Because of the low statistics the error is large. The high-frequency part of the spectral function of all data is shown to behave like Brownian fluctuations. This similar behavior of the time series analyzed can be understood because all three kinds of events are correlated since they have their origin in the solar activity.

The detrended analysis performed confirmed the existence of long-range correlations, for low frequencies, in all available data (the scaling coefficient $H_\alpha \approx 1$). Finally, the correspondence between the scaling exponent and the β exponent of the spectral analysis was confirmed with real data.

We warmly thank Professors Huner Fanchiotti and Sergio Sciutto for very useful discussions. We acknowledge the Pierre Auger Observatory for making the data publicly available and the Pierre Auger Collaboration Publication Committee for a critical reading of the text. Fermilab is operated by Fermi Research Alliance, LLC under Contract No. De-AC02-07CH11359 with the United States Department of Energy. C.A.G.C. and T.T. acknowledge partial support of ANPCyT of Argentina.

REFERENCES

Auger Collaboration 2004, Nucl. Instrum. Methods Phys. Res. A, 523, 50
Auger Scaler Data Online 2011, http://auger.colostate.edu/ED/scaler.php
Baillie, R. T. 1996, J. Economet., 73, 5
Bray, R. J., & Loughhead, R. E. 1979, Sunspots (New York: Dover)
Buldyrev, S. V., Goldberger, A. L., Havlin, S., et al. 1995, Phys. Rev. E, 51, 5084
Dasso, S., Asorey, H., & The Pierre Auger Collaboration 2012, Adv. Space Res., 49, 1563
Fanchiotti, H., Sciutto, S. J., García Canal, C. A., & Hojvat, H. 2004, Fractals, 12, 405
Hamilton, J. 1994, Time Series Analysis (Princeton, NJ: Princeton Univ. Press)
Heneghan, C., & McDarby, G. 2000, Phys. Rev. E, 62, 6103
Jensen, H. J. 1998, Self-Organized Criticality (Cambridge: Cambridge Univ. Press)
Kantelhardt, J. W., Zschiegner, S. A., Koscielny-Bunde, E., et al. 2002, Physica A, 316, 87
MacDonald, D. K. C. 1962, Noise and Fluctuations: An Introduction (New York: Wiley)
Matthaeus, W. H., & Goldstein, M. L. 1986, Phys. Rev. Lett., 57, 495
Neutron Monitor APTY 2011, Neutron Monitor JUNG 2011, http://www.nmdb.eu/?q=node/118#Apatity
Neutron Monitor Database 2011, http://www.nmdb.eu/nest/search.php
Neutron Monitor JUNG http://www.nmdb.eu/?q=node/12
Novikov, E., Novikov, A., Shannahoff-Khalsa, D., Schwartz, B., & Wright, J. 1997, Phys. Rev. E, 56, R2387
Peng, C.-K., Buldyrev, S. V., Havlin, S., et al. 1994, Phys. Rev. E, 49, 1685
Pierre Auger Collaboration, & Bertou, X. 2008, in Proc. 30th International Cosmic Ray Conference (ICRC 2007), ed. R. Caballero, J. C. D'Olivo, G. Medina-Tanco et al. (Mexico City: Univ. Nacional Autónoma de México), 441
Pierre Auger Observatory Collaboration 2011, J. Instrum., 6, 01003
Press, W. H. 1978, Comments Astrophys., 7, 103
SIDC-Team 2011, World Data Center for the Sunspot Index, Royal Observatory of Belgium, Monthly Report on the International Sunspot Number, Online Catalogue of the Sunspot Index: http://www.sidc.be/sunspot-data/, 2005–2011
Storini, M., et al. 2010, Rome Neutron Monitor, Supported by INAF/UNIRomaTre Collaboration, http://cr0.izmiran.rssi.ru/rome/
Van Vliet, C. M. 1991, Solid-State Electron., 34, 1
Voss, R. F., & Clarke, J. 1975, Nature, 258, 317